



HAL
open science

Evidence of Chlordecone Resurrection by Glyphosate in French West Indies

Pierre Sabatier, Charles Mottes, Nathalie Cottin, Olivier Evrard, Irina Comte, Christine Piot, Bastien Gay, Fabien Arnaud, Irène Lefevre, Anne-Lise Develle, et al.

► To cite this version:

Pierre Sabatier, Charles Mottes, Nathalie Cottin, Olivier Evrard, Irina Comte, et al.. Evidence of Chlordecone Resurrection by Glyphosate in French West Indies. *Environmental Science and Technology*, 2021, 25 (4), pp.2296-2306. 10.1021/acs.est.0c05207 . cea-03124787

HAL Id: cea-03124787

<https://cea.hal.science/cea-03124787>

Submitted on 29 Jan 2021

HAL is a multi-disciplinary open access archive for the deposit and dissemination of scientific research documents, whether they are published or not. The documents may come from teaching and research institutions in France or abroad, or from public or private research centers.

L'archive ouverte pluridisciplinaire **HAL**, est destinée au dépôt et à la diffusion de documents scientifiques de niveau recherche, publiés ou non, émanant des établissements d'enseignement et de recherche français ou étrangers, des laboratoires publics ou privés.

1 Evidence of chlordecone resurrection by glyphosate in

2 French West Indies

3 *Pierre Sabatier*^{†,*}, *Charles Mottes*^{‡,§}, *Nathalie Cottin*^{||}, *Olivier Evrard*[†], *Irina Comte*^{§,#},
4 *Christine Piot*^{||}, *Bastien Gay*^{†,||}, *Fabien Arnaud*[†], *Irène Lefevre*[†], *Anne-Lise Develle*[†], *Landry*
5 *Deffontaines*^{‡,§}, *Joanne Plet*^{‡,§}, *Magalie Lesueur-Jannoyer*^{‡,§}, *Jérôme Poulenard*[†]

6 [†]: Univ. Grenoble Alpes, Univ. Savoie Mont Blanc, CNRS, EDYTEM, LE Bourget du lac, France

7 [‡]: Cirad, UPR HortSys, F-97285 Le Lamentin, Martinique, France

8 [§]: HortSys, Geco, Univ Montpellier, CIRAD, Montpellier, France

9 ^{||}: Univ. Savoie Mont-Blanc, LCME, Le Bourget du Lac, France

10 [†]: Univ. Paris-Saclay, UVSQ, CEA, CNRS, LSCE/IPSL, F-91191, Gif-sur-Yvette, France

11 [#]: Cirad, UPR GECO, F-97130 Capesterre-Belle-Eau, Guadeloupe, France

12

13 **KEYWORDS** : Critical zone, Glyphosate, Chlordecone, Soil erosion, Banana crops, sediment

14 cores

15 **ABSTRACT**: The widespread use of pesticides in agriculture during the last several decades has

16 contaminated soils and different Critical Zone (CZ) compartments, defined as the area extended

17 from the top of the vegetation canopy to the groundwater table, and it integrates interactions of the

18 atmosphere, lithosphere, biosphere, and hydrosphere. However, the long-term fate, storage, and

19 transfer dynamics of persistent pesticides in CZ under a changing world remain poorly understood.

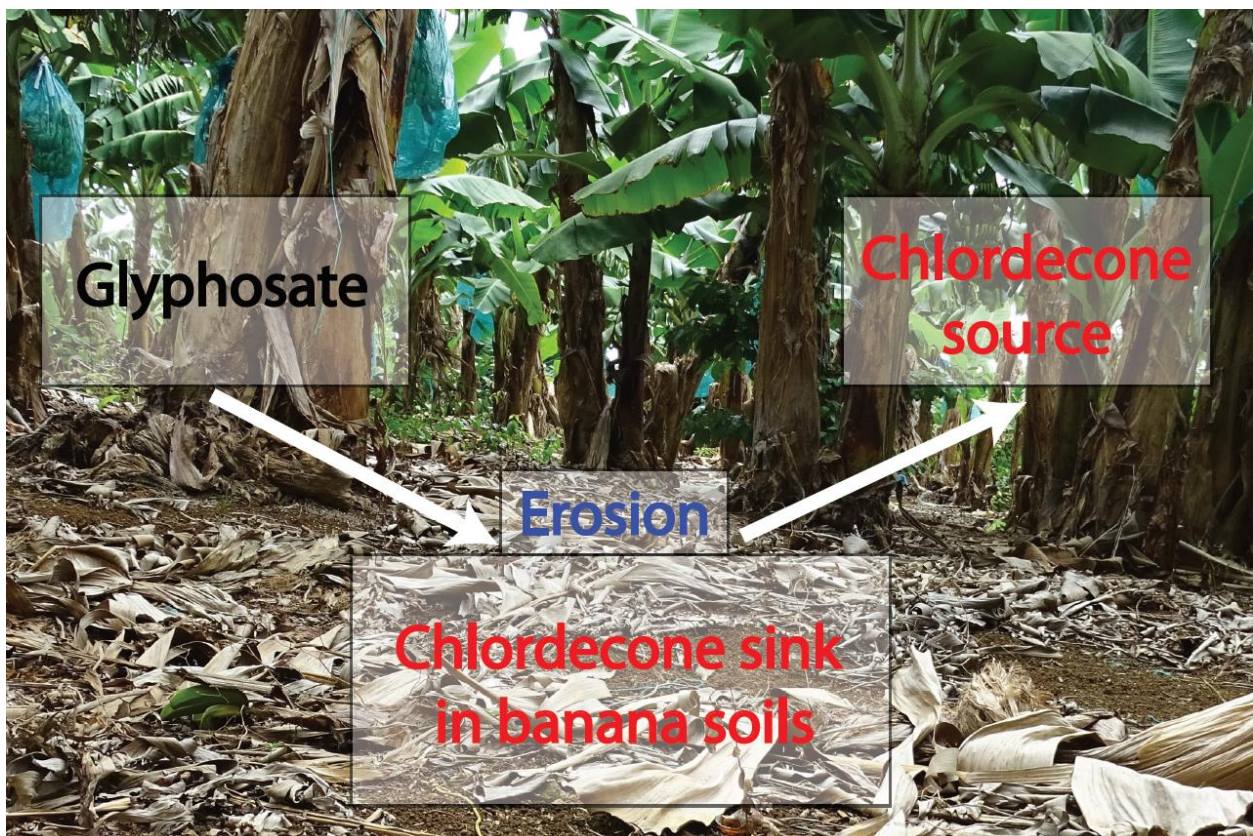
20 In the French West Indies (FWI), chlordecone (CLD), a toxic organochlorine insecticide, was

21 extensively applied to banana fields to control the banana weevil from 1972 to 1993, when it was

22 banned. Here, to understand CZ trajectories we apply a retrospective observation based on marine

23 sediment core analysis to monitor long-term CLD transfer, fate and consequences in Guadeloupe
24 and Martinique islands. Both CLD profiles show synchronous chronologies. We hypothesized that
25 the use of glyphosate, a postemergence herbicide, from the late 1990s onwards induced CZ
26 modification with an increase in soil erosion and led to the release of the stable CLD stored in the
27 soils of polluted fields. CLD fluxes drastically increased when glyphosate use began, leading to
28 widespread ecosystem contamination. As glyphosate is used globally, ecotoxicological risk
29 management strategies should consider how its application affects persistent pesticide storage in
30 soils, transfer dynamics and widespread contamination.

31 ABSTRACT IMAGE:



32

33 INTRODUCTION

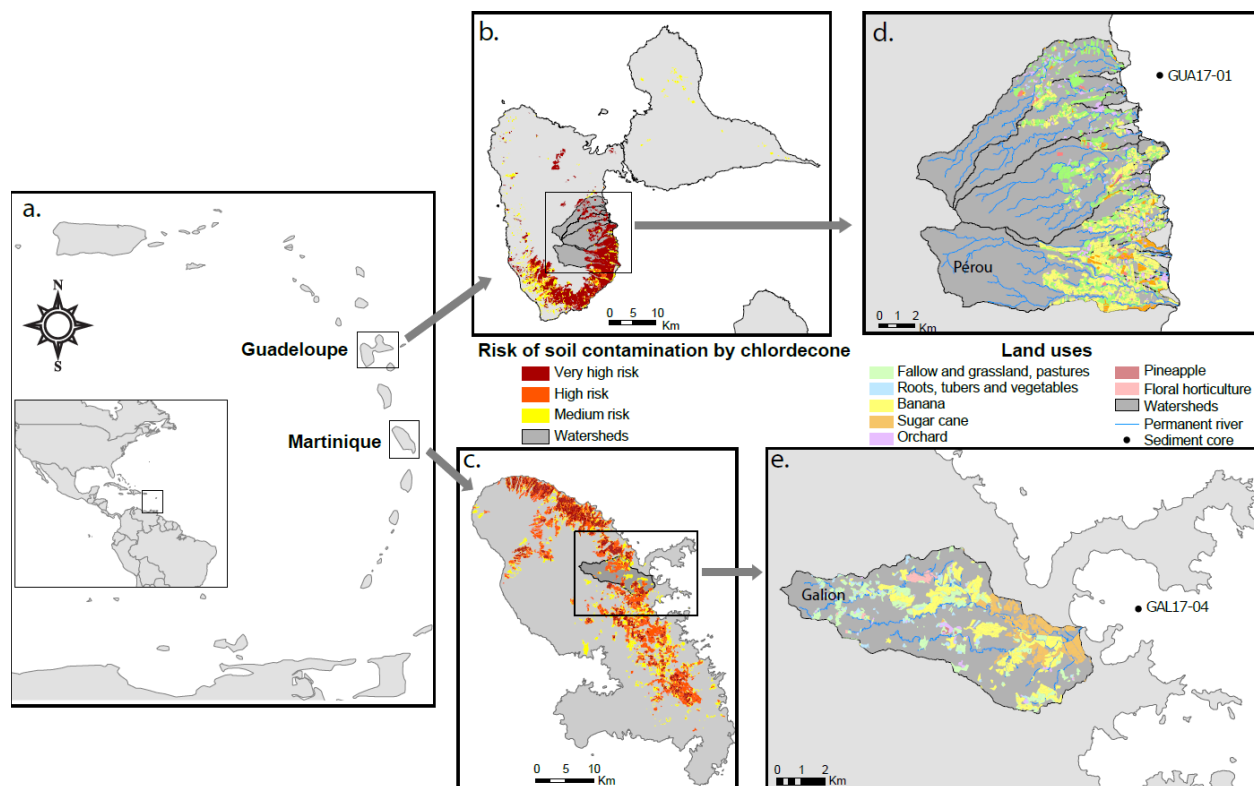
34 The Critical Zone (CZ) may be defined as the reactive skin of our planet within which most of its
35 coupled physical, chemical, biological and geological processes operating together to support life¹.
36 The emergence of human societies as a geological factor modified those subtle equilibria under
37 natural forcing (climate, tectonic)², resulting in unprecedented biodiversity loss, biogeochemical
38 disruptions and modifications of the erosion cycle³ leading to potential threats to the future of
39 humanity⁴. In recent decades, the sediment fluxes in CZ associated with the erosion of cultivated
40 soils have greatly increased in response to changes in agricultural practices⁵ such as deforestation,
41 overgrazing, tillage and unsuitable agricultural practices with the use of herbicides⁶. Over the last
42 several decades (last 70 years) is the use of many chemical substances to control disease
43 (fungicides), insect damage (Insecticides), and weed competition (herbicides) in cropland
44 dramatically rose⁷. Organochlorine insecticides such as dichlorodiphenyltrichloroethane (DDT,
45 $C_{14}H_9Cl_5$) or chlordecone (CLD, $C_{10}Cl_{10}O$) are classified as persistent organic pollutants (POPs)
46 by the Stockholm convention (<http://www.pops.int/>) but have been extensively used worldwide.
47 Their use has been progressively prohibited since the 1970s because of their biomagnification,
48 high toxicity, and long-term persistence in the environment. A well-known example is the
49 contamination from the Hopewell CLD production plant in the United States between 1965 and
50 1975 that resulted in high worker exposure and massive pollution of over 160 km of the James
51 River⁸, which lasted for several decades⁹. Despite CLD was extensively used worldwide, very few
52 studies document its adverse effects on environment excepted in the Caribbean area. In the French
53 West Indies (FWI, Fig. 1a) CLD was used to control the banana weevil during two periods: 1/
54 1972–1978 under the trade name Kepone[®], manufactured at Hopewell and 2/ 1982–1993 under
55 the trade name Curlone[®]. CLD was banned worldwide in 1992 except in the FWI where it has

56 been authorized until 1993 by the French government., However, CLD is still persistent in most
57 of CZ compartment such as soils¹⁰, crops¹¹, freshwater¹², coastal¹³ ecosystems until pelagic
58 cetaceans¹⁴, with potential for severe toxic effects to human populations¹⁵ with one of the highest
59 prostate cancer incidence in the world due to CLD exposure¹⁶ and the related highest mortality
60 rates¹⁷. These studies suggest that a significant amount of CLD is being transferred to the ocean,
61 raising the question of contamination provenance and its long-term environmental fate for
62 ecotoxicological management strategies.

63 In the FWI, interactions between agricultural practices such as CLD application (~3 kg/ha/yr),
64 tillage, plant cover, irrigation and pedoclimatic conditions lead to high variability in the
65 contamination level of soils^{18,19} (Fig. 1b, c). CLD persistence in soils is explained by its 1)
66 hydrophobicity, resulting in a high affinity for soil organic matter (high K_{oc} 2.5 to 20 m³.kg⁻¹)¹⁰;
67 2) physical sequestration in the fractal structure of soils containing allophanic clay, such as
68 Andosols²⁰, which are typical of the volcanic FWI; and 3) poor biodegradability under aerobic
69 conditions due to its chemical structure²¹. Depending on the soil type and considering negligible
70 CLD degradation, it was estimated that CLD could remain in soil for at least several decades and
71 up to centuries¹⁰. Thus, surface soil horizons act as reservoirs of CLD, gradually releasing this
72 chemical into groundwater^{19,22,23} or bound to soil particles eroded by surface runoff²⁴. Thus, if
73 erosion of cultivated soils increases in response to changes in agricultural practices, soils will be
74 converting from sinks to sources of pesticides. It has been demonstrated, through monitoring plots,
75 simulation experiments and retrospective observation that the massive use of postemergence
76 herbicides such as glyphosate since the late 1990s has a strong effect on soil erosion, as it acts on
77 grass development and leads to permanently bare soil, as has been shown in vineyards^{6,25}
78 clementine²⁶ and rubber plantations²⁷. The present study was designed in order to test the

79 hypothesis of enhanced CLD remobilisation due to glyphosate application through the erosion of
80 contaminated soils, as previously observed in vineyards with DDT remobilization⁶.

81 To test this hypothesis, in the context of intensive glyphosate application²⁸, we applied a
82 retrospective observation^{6,29,30} based on the analysis of marine sediment cores in order to monitor
83 long-term CLD transfer from watersheds. Indeed, CZ is submitted to processes that occur at
84 various time-scales which implies its trajectories must be documented over longer time-periods
85 much longer than direct observation experiments³¹. A retrospective observation hence allows to
86 extend into the past monitoring observations thanks to dated sediment cores and associated
87 proxies. In the present study, downcore contaminant profiles were associated with high-resolution
88 sedimentological and geochemical proxies. Short-lived radionuclides provide a precise core
89 chronology and the evolution of erosion patterns⁶. The two investigated watersheds were the Pérou
90 River²³ in Guadeloupe and the Galion River¹⁹ in Martinique (Fig. 1d, e). These watersheds present
91 high to very high CLD soil risk contamination (Fig. 1b, c). Both watersheds are mainly occupied
92 by banana and sugar cane plantations (Fig. 1d, e). Large cropped areas in the Galion watershed
93 belong to large farms, while Pérou farmers are mostly smallholders.



94

95 **Figure 1:** a, Map of the Caribbean island arc with the localization of two French islands
 96 (Guadeloupe and Martinique). b, c, Maps of Guadeloupe and Martinique showing the risk of soil
 97 contamination by chlordecone (CLD; very high, high and medium risk); the dark gray area
 98 indicates the study area. d, e, Localization of the studied watershed (dark gray) according to land
 99 use. Different colors indicate the types of crops, and banana plantations are indicated in yellow.
 100 The two sampled marine sediment cores GUA17-01 and GAL17-04 are indicated by black dots.
 101 Note that the sediment core from Guadeloupe (d) was not collected off the estuary of the monitored
 102 Pérou River due to the absence of fine sediment in the coastal zone at this location. Pérou
 103 (Guadeloupe) and Galion (Martinique) river watersheds (d, e) were also sampled for detailed
 104 information see Figure S1. Land uses data of 2017 made available by the French Directions of
 105 Agriculture and Forestry of Martinique and Guadeloupe (DAAF Martinique and Guadeloupe).

106 *Risk of soil contamination by chlordecone made available by Préfecture of Martinique and*
107 *Préfecture of Guadeloupe, for their design see* ^{19,32-34}.

108

109 **MATERIALS AND METHODS**

110 **Sampling.** A 1.13-m-long core registered as GAL17-04 (N° IGSN TOAE0000000573) was
111 collected in the Baie du Galion in Martinique (WGS84: 14.72801600; -60.91658800) at 15 m
112 below sea level on April 2017. A 1.33-m-long core registered as GUA17-01 (N° IGSN
113 TOAE0000000567) was collected in Petit Cul-de-Sac Marin in Guadeloupe (16.16857500; -
114 61.56900800) at 13.3 m below sea level on April 2017. Both cores were sampled using an Uwitec
115 gravity corer with a hammer from a small boat. Surface soil horizons were sampled on the Galion
116 (Martinique, n=44) and Pérou (Guadeloupe, n=35) watersheds under different soil types (Nitisol,
117 Andosol, Ferralsols) and land use contexts (different crop types, forest, river sediment, channel
118 bank), as illustrated in figure S1. At the Grand Galion gauging station, 2 floods were sampled on
119 19 December 2013 and on 23 December 2013. During both floods, 24 water samples (330 mL
120 each) were taken every 6 min with an automatic sampler (Sigma SD900) when the limnimetric
121 level of the river exceeded 80 cm (i.e., $1.85 \text{ m}^3 \cdot \text{s}^{-1}$). Using this protocol, each flood was sampled
122 for 2 h 24 min, with a 6 min resolution. Water discharges during the two floods were also measured
123 with a pressure sensor. The discharges of both floods were provided by DEAL (The French
124 Environment, Planning and Housing Department). By the end of each flood, 24 flasks had been
125 collected. For both floods, due to material availability and logistical constraints, we selected 18
126 flasks for particle filtration. The selection retained the maximum variations in water color among
127 the flasks and thereby the maximum variability in the particle content among the samples. Using

128 a vacuum pump and 0.7 μm fiberglass filters (Whatman cat no 1825-047), we separated the
129 dissolved fraction ($< 0.7 \mu\text{m}$) from the particulate fraction ($\geq 0.7 \mu\text{m}$) for each of the 18 flasks
130 collected during each flood. The particulate and dissolved fractions were analyzed for CLD at the
131 Laboratoire Départemental d'Analyses de la Drôme (LDA26), which is COFRAC (French
132 Accreditation Committee) accredited. The results are presented with a $\pm 30\%$ error interval, and
133 the limit of quantification was $0.01 \mu\text{g. L}^{-1}$ for the dissolved fraction and 10 ng.g^{-1} for the
134 particulate fraction. According to the analytical requirements of the laboratory for CLD analysis,
135 samples were pooled (Table S1) to obtain the minimum (0.5 g) amount of solid, but the samples
136 were kept separate according to the flood rise, flood peak and flood fall. The mass of sediment in
137 each composite sample varied between 0.510 g and 0.891 g, while the volume of water filtered
138 from the composite samples varied between 200 mL and 950 mL.

139 **Logging.** In the laboratory, the cores were split lengthwise, photographed, and logged in detail,
140 noting all physical sedimentary structures. The grain size distributions of both cores were
141 determined using a Malvern Mastersizer 2000 (Isterre) with a continuous interval of 2 cm and
142 ultrasound during measurements. Cores were also cut at 2-cm depth intervals, and a specific
143 volume was dried at 60°C for 4 days to determine the dry bulk density (DBD); then, the Loss Of
144 Ignition (LOI) of each interval was measured using the protocol of Heiri³⁵. The LOIs at 550°C and
145 950°C correspond to the percent of organic and carbonate contents of the sediment, respectively.
146 The noncarbonate igneous residue (NCIR, express in %) of each sample was obtained by removing
147 the LOI550 and LOI950 from the initial dry weight. The terrigenous mass accumulation was
148 calculated as $\text{NCIR} \times \text{DBD} \times \text{sedimentation rate}$, expressed in $\text{g.cm}^{-2}.\text{yr}^{-1}$. X-Ray Fluorescence
149 (XRF) analysis was performed on the surfaces of the split sediment cores, which had been covered
150 with 4- μm -thick Ultralene, at 2-mm intervals using an Avaatech core scanner (EDYTEM). The

151 geochemical data were obtained with various tube settings: 10 kV at 0.15 mA for 15 s for Al, Si,
152 S, K, Ca, Ti and Fe and 30 kV at 0.2 mA for 20 s for Cu, Zn, Br and Sr³⁶. 3 replicates were
153 measured every 10cm to estimate the standard deviation. Each individual power spectrum was
154 deconvoluted into relative components (intensities), expressed in counts per second. The principal
155 component analysis (PCA) was performed using R software.

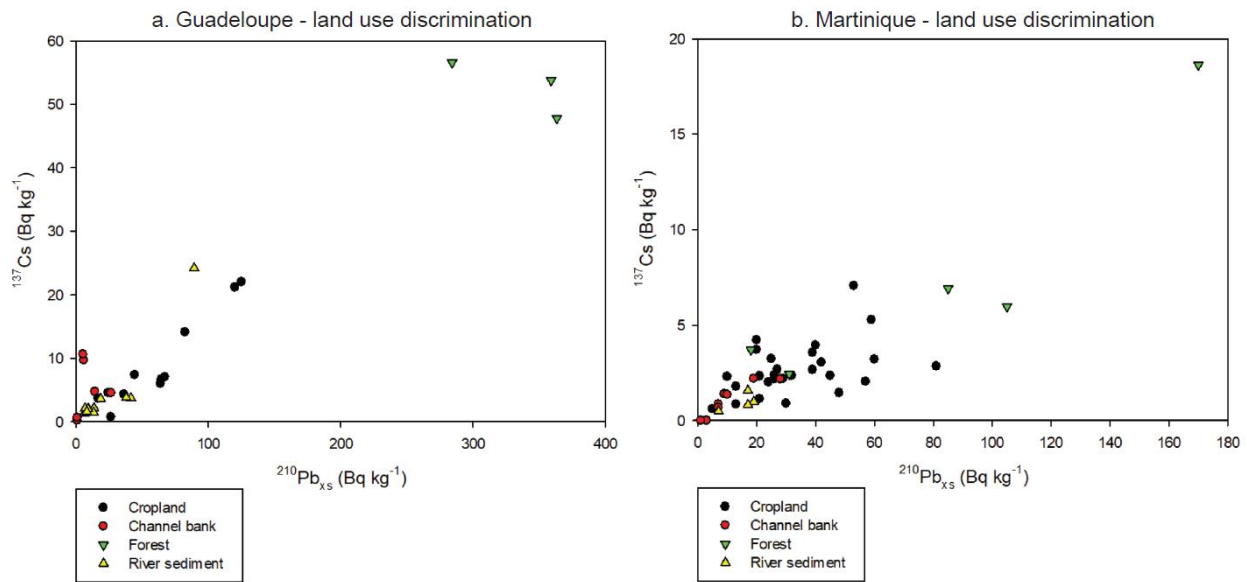
156 **Radionuclide measurements.** Surface soil horizons were sampled in the Galion (n=44) and Pérou
157 (n=35) watersheds at locations with different soil types and land use contexts, as illustrated in
158 figure S1, to assess whether erosion is an important mechanism on plantations through short-lived
159 radionuclide analyses. The two marine sediment cores collected in Petit Cul-de-Sac Marin
160 (GUA17-01, Guadeloupe) and Galion Bay (GAL17-04, Martinique) were analysed for short-lived
161 radionuclides to establish sediment chronology (Table S2 and S3). Prior to analyses, samples from
162 the watershed soils and core sediment were dried at 40°C for ~48 h, the watershed samples were
163 sieved to 2 mm, and all samples were ground to a fine powder in an agate mortar and pressed into
164 15 or 60 mL polyethylene containers depending on the quantity of material available for analysis.
165 Radionuclide activities were determined with gamma spectrometry using coaxial N- and P-type
166 HPGe detectors (Canberra/Ortec) at the Laboratoire des Sciences du Climat et de l'Environnement
167 (LSCE, Gif-sur-Yvette, France). The ¹³⁷Cs activity (half-life: 30.17 y) was measured from the
168 661.7 keV emission peak. The ²¹⁰Pb_{xs} activity (half-life: 22.3 y) was calculated by subtracting the
169 supported activity (determined by using two ²²⁶Ra daughters), the ²¹⁴Pb activity (average count
170 number at 295.2 and 351.9 keV) and the ²¹⁴Bi activity (609.3 keV) from the total ²¹⁰Pb activity
171 measured at 46.5 keV³⁷. Counting efficiencies and calibration were determined using certified
172 International Atomic Energy Agency (IAEA) standards (IAEA-444, 135, 375, RGU-1 and RGTh-
173 1) prepared in the same containers as the samples.

174 **Pesticide analysis.** Pesticide analyses were performed on samples from cores GUA17-01 (n=30)
175 and GAL17-04 (n=28) by an ALTHUS 30 ultraperformance liquid chromatography (UPLC)
176 system (Perkin Elmer, USA) coupled in tandem to a triple quadrupole mass spectrometer equipped
177 with an electrospray ionization (ESI) source (Perkin Elmer QSi 200). For CLD (Chlordecone)
178 and CLO (Chlordecol), 3 g of lyophilized dry sediment was extracted using an accelerated solvent
179 extraction system (ASE200, Dionex). The organic extract was then evaporated, purified and passed
180 through a 0.2 μm filter before analysis. The limit of detection (LOD, corresponding to a signal-to-
181 noise ratio of 3) and limit of quantification (LOQ, corresponding to a signal-to-noise ratio of 10)
182 were 0.22 $\text{ng}\cdot\text{mL}^{-1}$ and 0.67 $\text{ng}\cdot\text{mL}^{-1}$ for CLD and 0.1 $\text{ng}\cdot\text{mL}^{-1}$ and 0.3 $\text{ng}\cdot\text{mL}^{-1}$ for CLO,
183 respectively. For glyphosate and AMPA (Aminomethylphosphonic acid), 1 g of lyophilized dry
184 sediment was added to 10 mL of 0.5 M KOH and vortexed for 1 min. Glyphosate-2- $^{13}\text{C}^{15}\text{N}$ and
185 AMPA- $^{13}\text{C}^{15}\text{N}$ standard solutions were added as internal standards to a final concentration of
186 100 $\text{ng}\cdot\text{mL}^{-1}$ each. The extract was centrifuged, and the water extract was filtered through a 0.2 μm
187 nylon filter and analyzed immediately after preparation. The LOD and LOQ were 2 $\text{ng}\cdot\text{mL}^{-1}$ and 6
188 $\text{ng}\cdot\text{mL}^{-1}$ for glyphosate and 1 $\text{ng}\cdot\text{mL}^{-1}$ and 3 $\text{ng}\cdot\text{mL}^{-1}$ for AMPA, respectively. Detailed protocols
189 are presented in the supplementary material. Pesticides fluxes was calculated as $\text{DBD} \times$
190 sedimentation rate \times [pesticide] and expressed in $\text{mol}\cdot\text{g}\cdot\text{cm}^{-2}\cdot\text{y}^{-1}$.

191 **RESULTS AND DISCUSSION**

192 **On land erosion.** Samples under forest cover, found in upper catchment areas exposed to the
193 highest precipitation levels, were systematically enriched in ^{137}Cs and $^{210}\text{Pb}_{\text{xs}}$ relative to channel
194 bank samples (Fig. 2). The fallout radionuclide activities detected in cropland samples collected
195 on banana and sugarcane plantations showed intermediate levels between those detected in forests
196 and channel banks (Fig. 2). The results show that the sediment originates from a mix of cropland

197 (exposed to rainfall enriched in fallout radionuclides) and channel bank soils (sheltered from
 198 rainfall and fallout and depleted in radionuclides as demonstrated by Evrard et al. (2020)³⁸. These
 199 samples show that the banana and sugarcane plantations provide a significant supply of sediment
 200 to river systems on these islands through erosional processes.



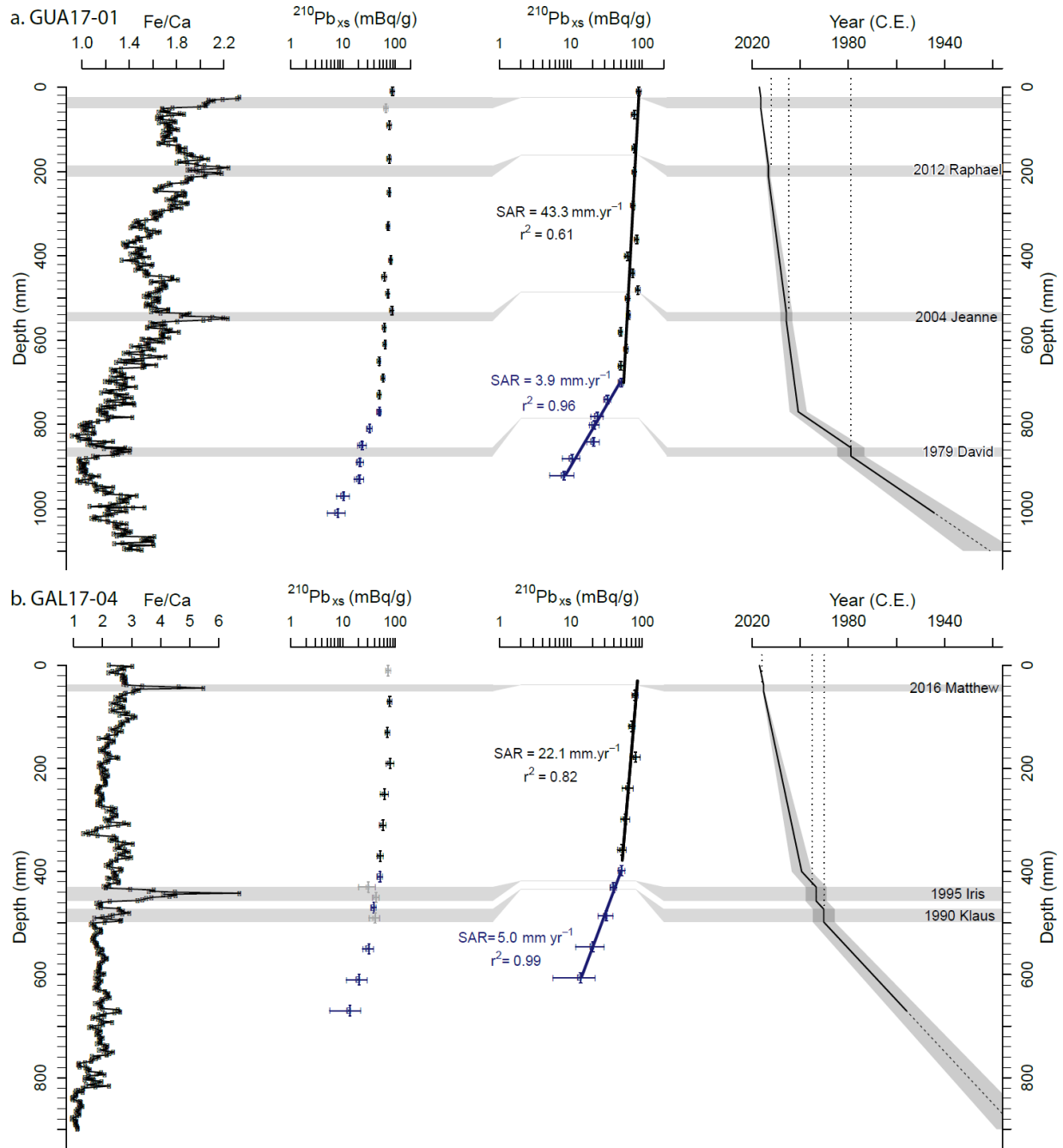
201
 202 **Figure 2: a, b,** $^{210}\text{Pb}_{\text{xs}}$ versus ^{137}Cs activities in the Pérou (Guadeloupe) and Galion (Martinique)
 203 river watersheds. Data are presented for the different land use conditions: cropland, forest, river
 204 sediment and channel bank. Forest samples are enriched in ^{137}Cs and $^{210}\text{Pb}_{\text{xs}}$, while channel banks
 205 are depleted in both radioisotopes.

206 **Sediment core and Chlordecone chronology.** The two marine sediment cores collected in Petit
 207 Cul-de-Sac Marin (GUA17-01, Guadeloupe) and Galion Bay (GAL17-04, Martinique) (Fig. 1d,
 208 e) were characterized in terms of their particle size, LOI, XRF mineral geochemistry and pesticide
 209 contents. Both cores contained relatively homogeneous olive-brown silt sediment. No noticeable
 210 variations in either the organic content or grain size distribution were observed (Fig. S2). These
 211 parameter variations hence could not have affected the absorption/degradation of pesticides within

212 the accumulated sediment⁶. PCA on XRF data (Fig. S3) showed two sediment end-member³⁹
213 inputs from the watershed, with organic matter and metallic pollutant contents and the marine
214 carbonate productivity. The geochemical data were in good agreement with the LOI indicating an
215 upward increase in terrigenous inputs from the watershed (reflected by the Fe content) while
216 carbonate productivity (reflected by the Ca content) decreased (Fig. S3). Accordingly, the Fe/Ca
217 ratio was used as a high-resolution proxy for the terrigenous fraction.

218 A chronological framework was established with the *serac* R package⁴⁰ from measurements of
219 short-lived radionuclides, constrained by the identification of historical hurricane event deposits
220 (Fig. 3, Table S2 and S3) as ¹³⁷Cs did not provide an interpretable profile in relation to its
221 desorption/migration in marine sediments⁴¹. The Fe/Ca data in the GUA17-01 and GAL17-04
222 cores led to the identification of 4 and 3 historical hurricane events, respectively, that caused heavy
223 precipitation in the region, as indicated by meteorological data (<http://pluiesextremes.meteo.fr/>),
224 which allow independent chronology validation. The sediment deposits triggered by these events
225 were considered as instantaneous and thus excluded from the construction of the age model, by
226 removing the depth interval and associated ²¹⁰Pb_{xs} data of each of these deposits^{40,42}. The
227 logarithmic plot of the event corrected ²¹⁰Pb_{xs} activity shows a general decrease, with two distinct
228 linear trends (black and dark blue Fig. 3). According to the “constant flux, constant sedimentation
229 rate” (CFCS) model⁴⁰ applied to each segment of the profile, the levels of ²¹⁰Pb_{xs} indicate drastic
230 increases in the sediment accumulation rate (SAR) from $3.9 \pm 0.6 \text{ mm.y}^{-1}$ to $43.3 \pm 9.5 \text{ mm.y}^{-1}$
231 and from $5.0 \pm 0.2 \text{ mm.y}^{-1}$ to $22.1 \pm 5.1 \text{ mm.y}^{-1}$ with synchronous changes in 2000 (uncertainty
232 range: 1996-2005) and 1999 (uncertainty: 1995-2004) in the GUA17-01 and GAL17-04 cores,
233 respectively (Fig. 3). These two age models are well constrained by the ages of the most intense
234 historical hurricanes that have hit both islands. This concomitant increase in sedimentation rates

235 in sediment records located more than 170 km away from each other might only be explained by
236 an increase in carbonate productivity in the marine system or by an increase in terrigenous inputs
237 from the watersheds. From these age models, the terrigenous mass accumulation was calculated
238 and interpreted as a proxy of soil erosion in the watershed, indicating that the erosion rate increased
239 10- and 4-fold on the basis of the GUA17601 and GAL17-04 cores, respectively (Fig. 4a, b). This
240 interpretation rules out the hypothesis of an increase in carbonate precipitation. It is further
241 supported by the observation of a synchronous increase in the Fe/Ca ratio for GUA core (Fig. 4a).
242 For the GAL core we observed a short time lag (corresponding to less than 2cm) between Fe/Ca
243 and terrigenous flux increase which could be related to sampling resolution (2cm for short-lived
244 radionuclides not in continuous versus continuous 2mm for XRF data) or to the influence of Iris
245 hurricane (Fig. 4b).



246

247 **Figure 3:** Chronology for the GUA17-01 (a) and GAL17-04 (b) cores with the Fe/Ca, $^{210}\text{Pb}_{\text{xs}}$
 248 activity, instantaneous event-corrected $^{210}\text{Pb}_{\text{xs}}$ activity and age model with uncertainties (gray
 249 area) realized with the serac R package⁴⁰. The dotted lines extending from the black lines indicate
 250 age model extrapolation. On the right part of this figure ages and names correspond to historical
 251 hurricanes.

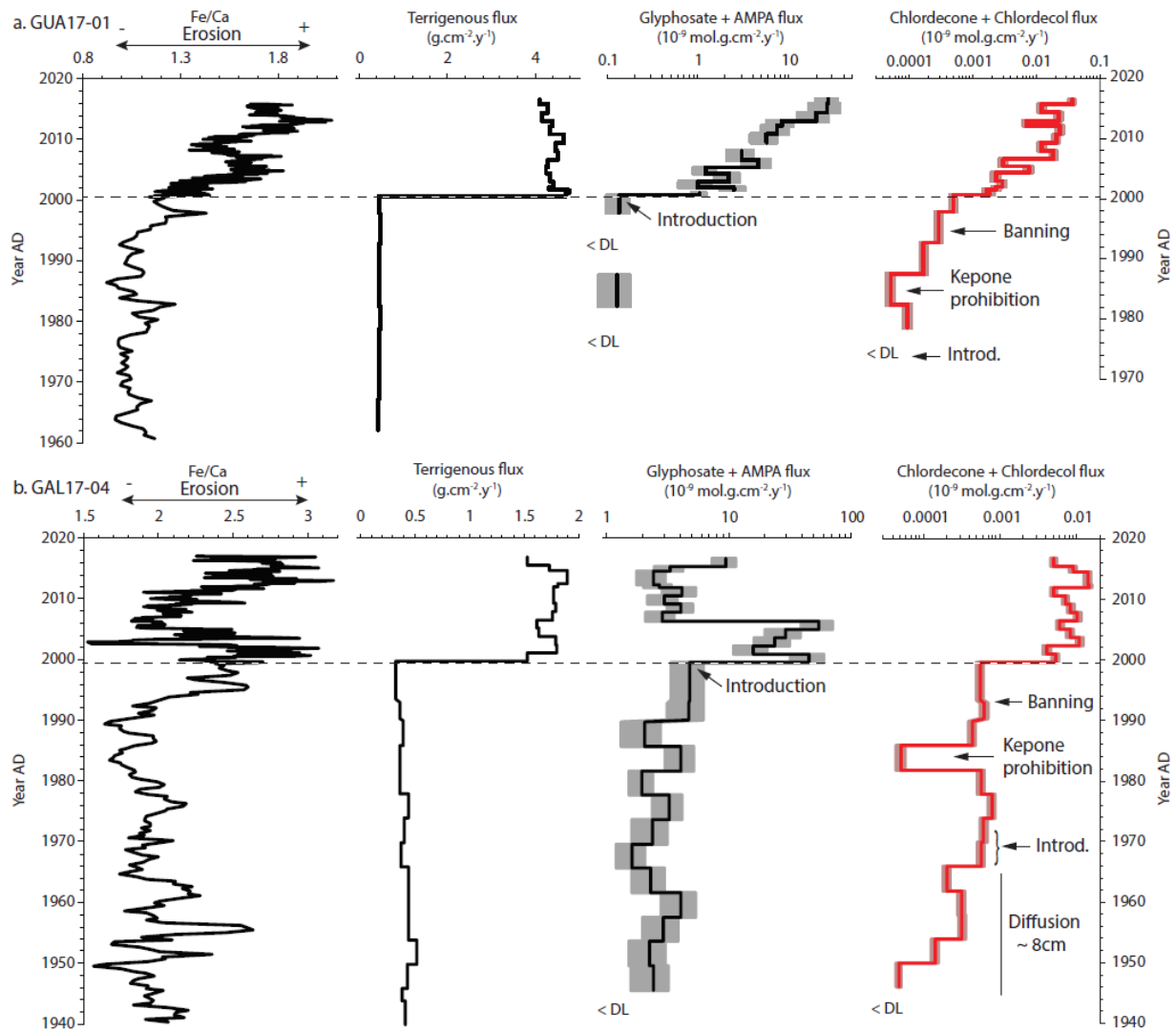
252

253 Pesticide temporal variations are presented in relation to age and displayed both in concentrations
254 (Fig. S4) and fluxes (Fig. 4). CLD and chlordecol (CLO, a CLD degradation product)
255 concentrations present similar profiles in both cores (Fig. S4) and were thus summed and expressed
256 as fluxes (Fig. 4) to account for the large increases in sedimentation rates. In GUA17-01, the
257 CLD+CLO flux is first detected in 1978 +/- 7 yr, just after the introduction of CLD in 1972 and
258 subsequently decreases, which could correspond to the period (1978-1982) between the
259 prohibition of Kepone[®] in the US and the approval of the license for the use of CLD in Curlone[®]
260 by the French authorities in late 1981. Then, the CLD+CLO flux increases, which continues even
261 after its ban in 1993. In 2000 +/-5 yr, we observed a 2-fold and more than 5-fold increase in the
262 CLD+CLO concentration and flux, respectively. In GAL17-04, CLD and CLO are first observed
263 in very low concentrations at 8 cm (1940-1955), before its introduction dated here at 1970 +/- 6 yr
264 (Fig. S4). This apparent preintroduction record of this compound may be explained by its possible
265 downward diffusion in sediment, as observed for other chlorinated molecules such as DDT⁶, or by
266 bioturbation in these shallow marine environments. Then, we observe a decrease in CLD+CLO
267 flux during the prohibition period, followed by an increase until the final ban. In 1999 +/-5 yr, we
268 detected a 2-fold and more than 10-fold increase in the concentration and flux, respectively.

269 Finally, between the period of maximum CLD use and the recent high flux, we noted more than
270 200-fold and 20-fold CLD+CLO flux increases in GUA17-01 and GAL17-04, respectively (Fig.
271 4). The CLO/CLD ratio is higher in the oldest part of the two sediment cores than in the most
272 recent sediment (Fig. S4) and in present-day soils in Martinique⁴³. CLO formation probably results
273 from the reduction of the CLD ketone group under anaerobic conditions⁴⁴, which are encountered

274 some centimeters below the water-sediment interface. This hypothesis is further supported by the
275 increase in CLO/CLD with depth suggesting to long-term CLD degradation within the sediment.

276 **Chlordecone transfer in critical zone.** CLD concentrations in soils surface layers of banana
277 plantations range from 500 to more than 2000 ng.g⁻¹ in the Galion watershed¹⁹ and from 30 to
278 more than 24000 ng.g⁻¹ in the Pérou watershed²³. This spatial variability in CLD soil pollution is
279 related both to the duration of the banana cropping period and soil characteristics¹⁰. Soils in which
280 banana was never planted did not contain any CLD¹⁹. Samples collected in 2002 at the mouth of
281 the Galion River contained 50 and < 10 ng.g⁻¹ CLD in suspended matter (>0.7 µm) and in sediment,
282 respectively⁴⁵, reflecting CLD dilution relative to soil concentrations. In comparison, the higher
283 CLD concentrations measured in the recent layers of the two studied sediment cores (1 to 2 ng.g⁻¹
284 ¹) were still lower than the concentrations in river samples. These differences could be explained
285 both by terrestrial particle dilution by other sediment sources such uncontaminated fields, channel
286 banks (Fig. 2) and marine sediments; and by particle size fractionation resulting in coarser
287 sediment fractions in cores (Fig. S2) and finer fractions in suspended matter (higher specific
288 surface area) collected in rivers and nearby river mouths⁴⁶.



289

290 **Figure 4:** Soil erosion proxies and pesticide flux chronology for Guadeloupe **a** and Martinique **b**:
 291 Erosion proxies with Fe/Ca and terrigenous fluxes compared to a pesticide chronology
 292 (logarithmic scale) reconstructed from the sum of glyphosate and aminomethylphosphonic acid
 293 (AMPA; glyphosate degradation product) fluxes and the sum of chlordecone and chlordocol (one
 294 of the chlordecone degradation products) fluxes. The horizontal dotted line corresponds to the
 295 large increase in sedimentation rate identified in response to a large erosion increase synchronous
 296 with glyphosate introduction and chlordecone flux increases. <DL indicates below the detection
 297 limit.

298 The collection of water samples during two low-intensity floods in December 2013 in the Galion
299 watershed permitted to assess the accumulated mass of transferred CLD in the dissolved and
300 particulate fractions (Fig. S5a, b). The CLD content in the particle-bound fraction ranged from 311
301 to 1059 ng.g⁻¹ (Fig. S5c, d). During both floods, the mass of CLD transferred by particles was
302 higher than that transferred in dissolved form (Fig. S5), indicating that soil erosion was an
303 important pathway for CLD transfer. In the case of very large floods, such as during storms or
304 cyclonic events, this process could transport huge amounts of CLD from land to sea and the
305 sediment. These results can be related to the erosion occurring in this watershed, identified by
306 short-lived radionuclide measurements in watershed samples (Fig. 2). We hence infer that erosion
307 of contaminated soil particles is a major CLD mass transfer process²⁴ which should therefore not
308 be neglected or considered minor, contrary to recent suggestions²².

309 **Critical zone erosion induced by Glyphosate.** The large CLD+CLO flux increases observed
310 around 1999/2000 in both cores are synchronous with a drastic rise in erosion fluxes (Fig. 4) and
311 thus probably have a common watershed origin. As the erosion increases synchronously in both
312 sites located on two different islands we can discard local phenomena such as road construction or
313 urban development. Thus, three main hypotheses could explain this observation: 1/ climate driver
314 with an increase in precipitation, 2/ change in mechanical practice on cropland with extensive
315 tillage or 3/ the extensive use of glyphosate leading to unprotected soil more sensitive to
316 precipitation-induced erosion. First we can discard the climate forcing as no significant
317 precipitation change can be identified from instrumental data during this period in this Caribbean
318 area⁴⁷. As these two watersheds have similar land use (Fig. 1d, e) and erosion characteristics of
319 banana and sugar cane fields (Fig. 2), we can hypothesize that a concomitant change in agricultural
320 practices caused this erosional increase. Since the early 1970s on banana plantations, the fields

321 were prepared for planting with heavy equipment to enable the planting of banana trees and the
322 drainage of water via ditches dug throughout the fields⁴⁸. These practices are known to contribute
323 to soil erosion but cannot explain its large increase more than 25 yrs later.

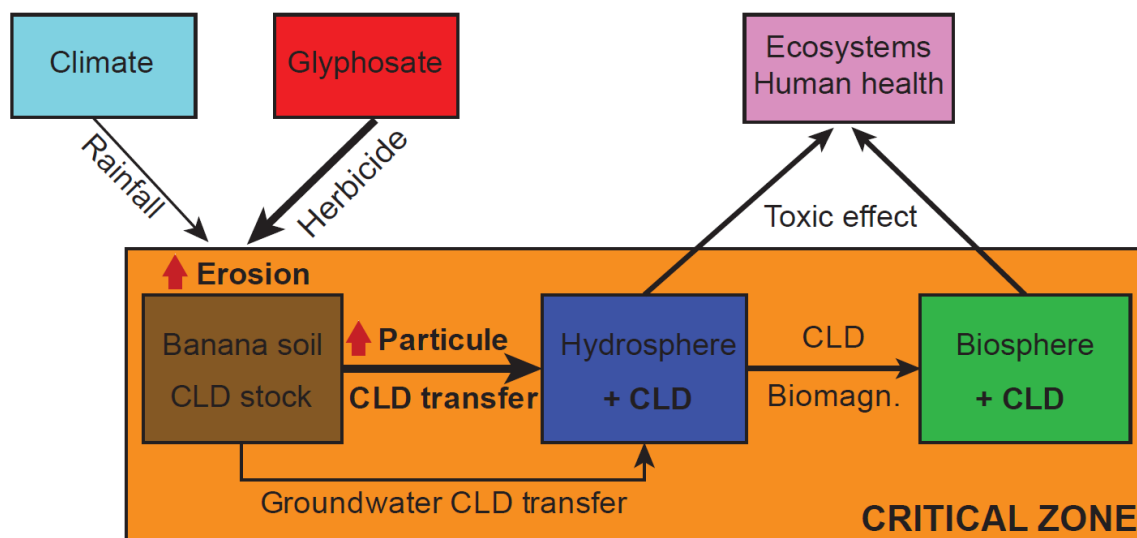
324 When these fluxes increase in the two cores, glyphosate and AMPA (glyphosate degradation
325 product) are detected in the GUA17-01 sediment for the first time, and both the concentrations and
326 flux considerably increase in the GAL17-04 sediment (Fig. S4). Glyphosate use began in 1974,
327 but few banana farmers (only large banana farms) probably used it from the early 1980s until 1997.
328 In 1997, the glyphosate price (Roundup) dropped, causing 90% of farmers to use it from that year
329 onwards. Glyphosate is still widely used in the FWI²⁸. This is in good agreement with the
330 emergence of this chemical in 1999/2000 +/- 5 yr in the two sediment chronologies (Fig. 4). In the
331 GAL17-04 core, the glyphosate and AMPA records start earlier (1950). Even if its use in some
332 large farms in the Galion watershed is not totally excluded, as the absence of such large farms in
333 the Pérou watershed points the diffusion of AMPA as the most probable explanations of downcore
334 migrations of these chemicals⁶ are diffusion and/or bioturbation processes. Since its earliest
335 appearance in GUA17-01, the glyphosate+AMPA flux continuously increased, while in GAL17-
336 04, after a drastic increase, this flux decreased in 2006.5 +/- 2.5 yr before re-increasing in the
337 uppermost layer (Fig. 4). This time corresponds to the entry into force of the French law on water
338 (2006-1772), which establishes an untreated area as a buffer around a watercourse, including
339 ditches. In Martinique, important surface drainage networks are present in banana fields. Stopping
340 glyphosate treatment would decrease the export of this chemical through the concentrated flows
341 in these ditches. However, glyphosate is still used in these fields, thereby probably maintaining
342 the transfer of soil particles contaminated by CLD. The difference between our study sites could

343 be linked to the fact that the large farms in the Galion watershed, which are monitored for good
344 practices, quickly adhered to the French law on water.

345 Even if the two watersheds are different in term of farm size, other important watershed
346 characteristics are the same: soils cover, type of cultures, climate. At both sites, we observed a
347 synchronous increase in CLD+CLO and erosional fluxes when glyphosate was first widely applied
348 to banana fields at the end of the 1990s. The application of glyphosate, which disrupts grass
349 development, has a strong effect on soil erosion as previous demonstrated through monitoring
350 plots, simulation experiments and retrospective observation^{6,25-27,49}. Other herbicides, such as
351 paraquat, and authorized in the French West Indies between 2003 and 2007, could have caused the
352 same issues. Paraquat was reported to be used along with glyphosate because of glyphosate
353 resistant plants⁵⁰ and intensively used in banana plantations in Latin America⁵¹. While glyphosate
354 is a systemic herbicide, paraquat and other herbicides used at the early 2000s on banana plantations
355 ²⁸ are either selective or non-systemic. As a result, they do not eliminate all plants on a field,
356 allowing them to recover. Paraquat, for instance is a non-selective but non-systemic herbicides. It
357 “burns” the leaves of plants while allowing plants to recover from stems or roots. Glyphosate acts
358 differently by killing the whole plants which leaves the soil bare and less-maintained by roots
359 leading to potential enhanced erosion rates. Erosion on bare soil might furthermore be amplified
360 by banana canopies, which exhibit high funneling ratios, favouring runoff even on soils with a
361 high infiltration rate such as Andosols, by localized rainfall redistribution and soil detachment by
362 concentrated flows⁵².

363 Putting all our observations together, we argue that the widespread use of a non-specific systemic
364 herbicide (glyphosate) since the late 1990s’ could be responsible of an unprecedented rise in soil
365 erosion and downstream of a major release of remnant CLD pesticides that were trapped in banana

366 fields soils since their banning in the Late-1990s' (Fig. 4). As such, we highlight that new
 367 agricultural practices may induce complex interactions in CZ dynamic converting soils from sinks
 368 to sources of formerly-used pesticides. This happened in FWI where CLD was probably
 369 resurrected by glyphosate-induced soil erosion (Fig. 5) just as in a French vineyard where DDT
 370 was resurrected by the same herbicide⁶. The eroded CLD-contaminated material was transported
 371 to the marine environment bound onto fine particles, where it became a source of contamination
 372 for marine organisms^{13,14,46} and a potential hazard to human health through seafood consumption
 373 (Fig. 5). This mechanism of old pesticides resurrection by glyphosate is now observed in banana
 374 plantation and vineyard, perhaps in no tillage agro systems glyphosate-induced soil erosion could
 375 be lower. We recommend future works to answer to this hypothesis. The retrospective observation
 376 applied here, allowed to reconstruct long-term CZ trajectories under human forcing, hence proving
 377 its strength in providing novel and complementary information to modern-day CZ observatories³¹.
 378



379

→ Increase process → Probable increase process
 → Constant process ↑ Positive feedback

380 **Figure 5:** *Critical Zone dynamics and responses in FWI relation to past (CLD) and modern*
381 *(Glyphosate) agricultural practices.*

382

383 Future studies of the environmental fate of pesticides in CZ should take into account these potential
384 pesticide–environment interactions from a long-term perspective. In terms of management options,
385 reducing soil erosion on cropland by limiting herbicide treatments would lead to the growth of
386 understory vegetation and ultimately result in the slower leaching of the pesticides stored in soils.
387 As glyphosate is used worldwide, it appears crucial that ecotoxicological risk assessments take
388 into account such mechanisms of remnant pesticide mobility in the environment through herbicide-
389 induced erosion.

390 ASSOCIATED CONTENT

391 Supporting Information.

392 Figure S1: Land use and sample in the investigated watersheds

393 Figure S2: Sedimentological and geochemical data in both cores

394 Figure S3: Biplot of the PCA of XRF geochemical data in both cores

395 Figure S4: Pesticide chronology expressed in concentration in both cores

396 Figure S5: Gauging station data during two flood events in the Galion watershed

397 Detailed pesticide analysis protocols

398 AUTHOR INFORMATION

399 Corresponding Author

400 * corresponding author : pierre.sabatier@univ-smb.fr <https://orcid.org/0000-0002-9620-1514>

401 Author Contributions

402 P.S., C.M., I.C., J.P. and O.E. conceived and designed the study. Fieldwork sampling were
403 performed by C.M., I.C., J.P., O.E., L.D. for soil sampling, P.S. and F.A. for coring and J.P., M.L.J.
404 and C.M. for water collecting. P.S., N.C., C.P., B.G., O.E., I.L. and A.L.D. performed the analyses.
405 P.S. wrote the first draft of the manuscript, with subsequent contribution by all the authors.

406 Funding Sources

407 This project EFFLUANT (EFFet à Long terme de l'Utilisation des pesticides aux ANtilles
408 françaises: pollution et érosion) was co-funded by the EC2CO/ BIOHEFECT structural action of
409 INSU/CNRS and the Labex DRIIHM, French programme "Investissements d'Avenir" (ANR-11-
410 LABX-0010), which is managed by the ANR, and the OHM Littoral Caraïbe

411 ACKNOWLEDGMENT

412 We thank the French Water Office of Martinique for their financial support of the flood sampling,
413 as well as the farmers of the two watersheds that gave us access to their fields for soil sampling.
414 The authors thank the Laboratoire Souterrain de Modane (LSM) facilities for the gamma
415 spectrometry measurements and Environnement, Dynamique et Territoires de Montagne for the
416 X-ray fluorescence analyses. The authors wish to thank the editor Jennifer A. Field and the three
417 anonymous reviewer who brought comments which greatly improved the original manuscript.

418 ABBREVIATIONS

419 CLD: Chlordecone

420 CLO: Chlordecol

421 AMPA: Aminomethylphosphonic acid

422 DDT: Dichlorodiphenyltrichloroethane

423 FWI : French west indies

424 CZ: Critical zone

425 LOI : Loss of ignition

426 XRF : X-ray fluorescence

427 DBD : Dry bulk density

428 NCIR : Noncarbonate igneous residue

429 CFCS: Constant flux, constant sedimentation rate

430 PCA : Principal component analysis

431 REFERENCES

- 432 (1) Banwart, S.; J., C.; G., G.; D., S.; White, T.; Anderson, S.; A., A.; Bernasconi, S.; Brantley,
433 S.; Chadwick, O.; W.L.E., D.; Duffy, C.; Goldhaber, M.; Lehnert, K.; Nikolaidis, N.;
434 Ragnarsdottir, K. *Sustaining Earth's Critical Zone Basic Science and Interdisciplinary*
435 *Solutions for Global Challenges*; 2013.
- 436 (2) Brantley, S. L.; Goldhaber, M. B.; Ragnarsdottir, K. V. Crossing Disciplines and Scales to
437 Understand the Critical Zone. *Elements* **2007**, *3* (5), 307–314.
438 <https://doi.org/10.2113/gselements.3.5.307>.
- 439 (3) Syvitski, J. P. M. Impact of Humans on the Flux of Terrestrial Sediment to the Global
440 Coastal Ocean. *Science* **2005**, *308* (5720), 376–380.
441 <https://doi.org/10.1126/science.1109454>.
- 442 (4) Steffen, W.; Richardson, K.; Rockstrom, J.; Cornell, S. E.; Fetzer, I.; Bennett, E. M.; Biggs,
443 R.; Carpenter, S. R.; de Vries, W.; de Wit, C. A.; Folke, C.; Gerten, D.; Heinke, J.; Mace,
444 G. M.; Persson, L. M.; Ramanathan, V.; Reyers, B.; Sorlin, S. Planetary Boundaries:
445 Guiding Human Development on a Changing Planet. *Science* **2015**, *347* (6223), 1259855–
446 1259855. <https://doi.org/10.1126/science.1259855>.
- 447 (5) Borrelli, P.; Robinson, D. A.; Fleischer, L. R.; Lugato, E.; Ballabio, C.; Alewell, C.;
448 Meusburger, K.; Modugno, S.; Schütt, B.; Ferro, V.; Bagarello, V.; Oost, K. V.;
449 Montanarella, L.; Panagos, P. An Assessment of the Global Impact of 21st Century Land
450 Use Change on Soil Erosion. *Nature Communications* **2017**, *8* (1).
451 <https://doi.org/10.1038/s41467-017-02142-7>.
- 452 (6) Sabatier, P.; Poulénard, J.; Fanget, B.; Reyss, J.-L.; Develle, A.-L.; Wilhelm, B.; Ployon,
453 E.; Pignol, C.; Naffrechoux, E.; Dorioz, J.-M.; Montuelle, B.; Arnaud, F. Long-Term
454 Relationships among Pesticide Applications, Mobility, and Soil Erosion in a Vineyard

- 455 Watershed. *Proceedings of the National Academy of Sciences* **2014**, *111* (44), 15647–15652.
456 <https://doi.org/10.1073/pnas.1411512111>.
- 457 (7) Gianessi, L. P. The Increasing Importance of Herbicides in Worldwide Crop Production:
458 The Increasing Importance of Herbicides. *Pest Management Science* **2013**, *69* (10), 1099–
459 1105. <https://doi.org/10.1002/ps.3598>.
- 460 (8) Huggett, R. J.; Bender, M. E. Kepone in the James River. *Environmental Science &*
461 *Technology* **1980**, *14* (8), 918–923. <https://doi.org/10.1021/es60168a001>.
- 462 (9) Luellen, D. R.; Vadas, G. G.; Unger, M. A. Kepone in James River Fish: 1976–2002.
463 *Science of The Total Environment* **2006**, *358* (1–3), 286–297.
464 <https://doi.org/10.1016/j.scitotenv.2005.08.046>.
- 465 (10) Cabidoche, Y.-M.; Achard, R.; Cattán, P.; Clermont-Dauphin, C.; Massat, F.; Sansoulet, J.
466 Long-Term Pollution by Chlordecone of Tropical Volcanic Soils in the French West Indies:
467 A Simple Leaching Model Accounts for Current Residue. *Environmental Pollution* **2009**,
468 *157* (5), 1697–1705. <https://doi.org/10.1016/j.envpol.2008.12.015>.
- 469 (11) Clostre, F.; Letourmy, P.; Lesueur-Jannoyer, M. Organochlorine (Chlordecone) Uptake by
470 Root Vegetables. *Chemosphere* **2015**, *118*, 96–102.
471 <https://doi.org/10.1016/j.chemosphere.2014.06.076>.
- 472 (12) Coat, S.; Monti, D.; Legendre, P.; Bouchon, C.; Massat, F.; Lepoint, G. Organochlorine
473 Pollution in Tropical Rivers (Guadeloupe): Role of Ecological Factors in Food Web
474 Bioaccumulation. *Environmental Pollution* **2011**, *159* (6), 1692–1701.
475 <https://doi.org/10.1016/j.envpol.2011.02.036>.
- 476 (13) Dromard, C. R.; Guéné, M.; Bouchon-Navaro, Y.; Lemoine, S.; Cordonnier, S.; Bouchon,
477 C. Contamination of Marine Fauna by Chlordecone in Guadeloupe: Evidence of a Seaward
478 Decreasing Gradient. *Environmental Science and Pollution Research* **2018**, *25* (15), 14294–
479 14301. <https://doi.org/10.1007/s11356-017-8924-6>.
- 480 (14) Méndez-Fernandez, P.; Kiszka, J. J.; Heithaus, M. R.; Beal, A.; Vandersarren, G.; Caurant,
481 F.; Spitz, J.; Taniguchi, S.; Montone, R. C. From Banana Fields to the Deep Blue:
482 Assessment of Chlordecone Contamination of Oceanic Cetaceans in the Eastern Caribbean.
483 *Marine Pollution Bulletin* **2018**, *137*, 56–60.
484 <https://doi.org/10.1016/j.marpolbul.2018.10.012>.
- 485 (15) Multigner, L.; Kadhel, P.; Rouget, F.; Blanchet, P.; Cordier, S. Chlordecone Exposure and
486 Adverse Effects in French West Indies Populations. *Environmental Science and Pollution*
487 *Research* **2016**, *23* (1), 3–8. <https://doi.org/10.1007/s11356-015-4621-5>.
- 488 (16) Multigner, L.; Ndong, J. R.; Giusti, A.; Romana, M.; Delacroix-Maillard, H.; Cordier, S.;
489 Jégou, B.; Thome, J. P.; Blanchet, P. Chlordecone Exposure and Risk of Prostate Cancer.
490 *Journal of Clinical Oncology* **2010**, *28* (21), 3457–3462.
491 <https://doi.org/10.1200/JCO.2009.27.2153>.
- 492 (17) Taitt, H. E. Global Trends and Prostate Cancer: A Review of Incidence, Detection, and
493 Mortality as Influenced by Race, Ethnicity, and Geographic Location. *American Journal of*
494 *Men's Health* **2018**, *12* (6), 1807–1823. <https://doi.org/10.1177/1557988318798279>.
- 495 (18) Clostre, F.; Lesueur-Jannoyer, M.; Achard, R.; Letourmy, P.; Cabidoche, Y.-M.; Cattán, P.
496 Decision Support Tool for Soil Sampling of Heterogeneous Pesticide (Chlordecone)
497 Pollution. *Environmental Science and Pollution Research* **2014**, *21* (3), 1980–1992.
498 <https://doi.org/10.1007/s11356-013-2095-x>.
- 499 (19) Della Rossa, P.; Jannoyer, M.; Mottes, C.; Plet, J.; Bazizi, A.; Arnaud, L.; Jestin, A.;
500 Woignier, T.; Gaude, J.-M.; Cattán, P. Linking Current River Pollution to Historical

- 501 Pesticide Use: Insights for Territorial Management? *Science of The Total Environment*
502 **2017**, 574, 1232–1242. <https://doi.org/10.1016/j.scitotenv.2016.07.065>.
- 503 (20) Woignier, T.; Clostre, F.; Macarie, H.; Jannoyer, M. Chlordecone Retention in the Fractal
504 Structure of Volcanic Clay. *Journal of Hazardous Materials* **2012**, 241–242, 224–230.
505 <https://doi.org/10.1016/j.jhazmat.2012.09.034>.
- 506 (21) Fernández-Bayo, J. D.; Saison, C.; Voltz, M.; Disko, U.; Hofmann, D.; Berns, A. E.
507 Chlordecone Fate and Mineralisation in a Tropical Soil (Andosol) Microcosm under
508 Aerobic Conditions. *Science of The Total Environment* **2013**, 463–464, 395–403.
509 <https://doi.org/10.1016/j.scitotenv.2013.06.044>.
- 510 (22) Cattan, P.; Charlier, J.-B.; Clostre, F.; Letourmy, P.; Arnaud, L.; Gresser, J.; Jannoyer, M.
511 A Conceptual Model of Organochlorine Fate from a Combined Analysis of Spatial and Mid-
512 to Long-Term Trends of Surface and Ground Water Contamination in Tropical Areas
513 (FWI). *Hydrology and Earth System Sciences* **2019**, 23 (2), 691–709.
514 <https://doi.org/10.5194/hess-23-691-2019>.
- 515 (23) Crabit, A.; Cattan, P.; Colin, F.; Voltz, M. Soil and River Contamination Patterns of
516 Chlordecone in a Tropical Volcanic Catchment in the French West Indies (Guadeloupe).
517 *Environmental Pollution* **2016**, 212, 615–626.
518 <https://doi.org/10.1016/j.envpol.2016.02.055>.
- 519 (24) Mottes, C.; Charlier, J.-B.; Rocle, N.; Gresser, J.; Lesueur-Jannoyer, M.; Cattan, P. From
520 Fields to Rivers Chlordecone Transfer in Water. In *Crisis management of chronic pollution:
521 contaminated soil and human health*; Boca Raton : CRC Press, 2016; pp 121–130.
- 522 (25) Blavet, D.; De Noni, G.; Le Bissonnais, Y.; Leonard, M.; Maillo, L.; Laurent, J. Y.;
523 Asseline, J.; Leprun, J. C.; Arshad, M. A.; Roose, E. Effect of Land Use and Management
524 on the Early Stages of Soil Water Erosion in French Mediterranean Vineyards. *Soil and
525 Tillage Research* **2009**, 106 (1), 124–136. <https://doi.org/10.1016/j.still.2009.04.010>.
- 526 (26) Keesstra, S. D.; Rodrigo-Comino, J.; Novara, A.; Giménez-Morera, A.; Pulido, M.; Di
527 Prima, S.; Cerdà, A. Straw Mulch as a Sustainable Solution to Decrease Runoff and Erosion
528 in Glyphosate-Treated Clementine Plantations in Eastern Spain. An Assessment Using
529 Rainfall Simulation Experiments. *CATENA* **2019**, 174, 95–103.
530 <https://doi.org/10.1016/j.catena.2018.11.007>.
- 531 (27) Liu, H.; Blagodatsky, S.; Giese, M.; Liu, F.; Xu, J.; Cadisch, G. Impact of Herbicide
532 Application on Soil Erosion and Induced Carbon Loss in a Rubber Plantation of Southwest
533 China. *CATENA* **2016**, 145, 180–192. <https://doi.org/10.1016/j.catena.2016.06.007>.
- 534 (28) Mottes, C.; Lesueur Jannoyer, M.; Le Bail, M.; Guéné, M.; Carles, C.; Malézieux, E.
535 Relationships between Past and Present Pesticide Applications and Pollution at a Watershed
536 Outlet: The Case of a Horticultural Catchment in Martinique, French West Indies.
537 *Chemosphere* **2017**, 184, 762–773. <https://doi.org/10.1016/j.chemosphere.2017.06.061>.
- 538 (29) Auer, M. T.; Johnson, N. A.; Penn, M. R.; Effler, S. W. Pollutant Sources, Depositional
539 Environment, and the Surficial Sediments of Onondaga Lake, New York. *Journal of
540 Environmental Quality* **1996**, 25 (1), 46–55.
541 <https://doi.org/10.2134/jeq1996.00472425002500010006x>.
- 542 (30) Barra, R.; Cisternas, M.; Urrutia, R.; Pozo, K.; Pacheco, P.; Parra, O.; Focardi, S. First
543 Report on Chlorinated Pesticide Deposition in a Sediment Core from a Small Lake in
544 Central Chile. *Chemosphere* **2001**, 45 (6–7), 749–757. [https://doi.org/10.1016/S0045-6535\(01\)00146-1](https://doi.org/10.1016/S0045-6535(01)00146-1).

- 546 (31) Gaillardet, J.; Braud, I.; Hankard, F.; Anquetin, S.; Bour, O.; Dorfliger, N.; de Dreuzy, J.
547 R.; Galle, S.; Galy, C.; Gogo, S.; Gourcy, L.; Habets, F.; Laggoun, F.; Longuevergne, L.;
548 Le Borgne, T.; Naaim-Bouvet, F.; Nord, G.; Simonneaux, V.; Six, D.; Tallec, T.; Valentin,
549 C.; Abril, G.; Allemand, P.; Arènes, A.; Arfib, B.; Arnaud, L.; Arnaud, N.; Arnaud, P.;
550 Audry, S.; Comte, V. B.; Batiot, C.; Battais, A.; Bellot, H.; Bernard, E.; Bertrand, C.;
551 Bessière, H.; Binet, S.; Bodin, J.; Bodin, X.; Boithias, L.; Bouchez, J.; Boudevillain, B.;
552 Moussa, I. B.; Branger, F.; Braun, J. J.; Brunet, P.; Caceres, B.; Calmels, D.; Cappelaere,
553 B.; Celle-Jeanton, H.; Chabaux, F.; Chalikakis, K.; Champollion, C.; Copard, Y.; Cotel, C.;
554 Davy, P.; Deline, P.; Delrieu, G.; Demarty, J.; Dessert, C.; Dumont, M.; Emblanch, C.;
555 Ezzahar, J.; Estèves, M.; Favier, V.; Faucheux, M.; Filizola, N.; Flammarion, P.; Floury, P.;
556 Fovet, O.; Fournier, M.; Francez, A. J.; Gandois, L.; Gascuel, C.; Gayer, E.; Genthon, C.;
557 Gérard, M. F.; Gilbert, D.; Gouttevin, I.; Grippa, M.; Gruau, G.; Jardani, A.; Jeanneau, L.;
558 Join, J. L.; Jourde, H.; Karbou, F.; Labat, D.; Lagadeuc, Y.; Lajeunesse, E.; Lastennet, R.;
559 Lavado, W.; Lawin, E.; Lebel, T.; Le Bouteiller, C.; Legout, C.; Lejeune, Y.; Le Meur, E.;
560 Le Moigne, N.; Lions, J.; Lucas, A.; Malet, J. P.; Marais-Sicre, C.; Maréchal, J. C.; Marlin,
561 C.; Martin, P.; Martins, J.; Martinez, J. M.; Massei, N.; Mauclerc, A.; Mazzilli, N.; Molénat,
562 J.; Moreira-Turcq, P.; Mougou, E.; Morin, S.; Ngoupayou, J. N.; Panthou, G.; Peugeot, C.;
563 Picard, G.; Pierret, M. C.; Porel, G.; Probst, A.; Probst, J. L.; Rabatel, A.; Raclot, D.;
564 Ravanel, L.; Rejiba, F.; René, P.; Ribolzi, O.; Riotte, J.; Rivière, A.; Robain, H.; Ruiz, L.;
565 Sanchez-Perez, J. M.; Santini, W.; Sauvage, S.; Schoeneich, P.; Seidel, J. L.; Sekhar, M.;
566 Sengtaheuanghoung, O.; Silvera, N.; Steinmann, M.; Soruco, A.; Tallec, G.; Thibert, E.;
567 Lao, D. V.; Vincent, C.; Viville, D.; Wagnon, P.; Zitouna, R. OZCAR: The French Network
568 of Critical Zone Observatories. *Vadose Zone Journal* **2018**, *17* (1), 180067.
569 <https://doi.org/10.2136/vzj2018.04.0067>.
- 570 (32) J.F. Desprats; Comte, J. P.; Charbier, C. Cartographie du risque de pollution des sols de
571 Martinique par les organochlorés. Rapport Phase 3. BRGM RP 53262 2004.
- 572 (33) Tillieut, O. Cartographie de La Pollution Des Sols de Guadeloupe Par La Chlordécone :
573 Rapport Technique 2005-2006. DAF971, SPV 2006 2005.
- 574 (34) Rochette, R.; Bonnal, V.; Andrieux, P.; Cattan, P. Analysis of Surface Water Reveals Land
575 Pesticide Contamination: An Application for the Determination of Chlordecone-Polluted
576 Areas in Guadeloupe, French West Indies. *Environmental Science and Pollution Research*
577 **2020**. <https://doi.org/10.1007/s11356-020-10718-y>.
- 578 (35) Heiri, O.; Lotter, A. F.; Lemcke, G. Loss on Ignition as a Method for Estimating Organic
579 and Carbonate Content in Sediments: Reproducibility and Comparability of Results.
580 *Journal of Paleolimnology* **2001**, *25* (1), 101–110.
581 <https://doi.org/10.1023/A:1008119611481>.
- 582 (36) Richter, T. O.; van der Gaast, S.; Koster, B.; Vaars, A.; Gieles, R.; de Stigter, H. C.; De
583 Haas, H.; van Weering, T. C. E. The Avaatech XRF Core Scanner: Technical Description
584 and Applications to NE Atlantic Sediments. *Geological Society, London, Special*
585 *Publications* **2006**, *267* (1), 39–50. <https://doi.org/10.1144/GSL.SP.2006.267.01.03>.
- 586 (37) Le Gall, M.; Evrard, O.; Foucher, A.; Laceby, J. P.; Salvador-Blanes, S.; Manière, L.;
587 Lefèvre, I.; Cerdan, O.; Ayrault, S. Investigating the Temporal Dynamics of Suspended
588 Sediment during Flood Events with ⁷Be and ²¹⁰Pbxs Measurements in a Drained Lowland
589 Catchment. *Scientific Reports* **2017**, *7* (1). <https://doi.org/10.1038/srep42099>.

- 590 (38) Evrard, O.; Chaboche, P.-A.; Ramon, R.; Foucher, A.; Lacey, J. P. A Global Review of
591 Sediment Source Fingerprinting Research Incorporating Fallout Radiocesium (¹³⁷Cs).
592 *Geomorphology* **2020**, *362*, 107103. <https://doi.org/10.1016/j.geomorph.2020.107103>.
- 593 (39) Sabatier, P.; Dezileau, L.; Briquieu, L.; Colin, C.; Siani, G. Clay Minerals and Geochemistry
594 Record from Northwest Mediterranean Coastal Lagoon Sequence: Implications for
595 Paleostorm Reconstruction. *Sedimentary Geology* **2010**, *228* (3–4), 205–217.
596 <https://doi.org/10.1016/j.sedgeo.2010.04.012>.
- 597 (40) Bruel, R.; Sabatier, P. Serac: An R Package for Shortlived RADionuclide Chronology of
598 Recent Sediment Cores. *Journal of Environmental Radioactivity* **2020**, *225*, 106449.
599 <https://doi.org/10.1016/j.jenvrad.2020.106449>.
- 600 (41) Delaval, A.; Duffa, C.; Radakovitch, O. A Review on Cesium Desorption at the Freshwater-
601 Seawater Interface. *Journal of Environmental Radioactivity* **2020**, *218*, 106255.
602 <https://doi.org/10.1016/j.jenvrad.2020.106255>.
- 603 (42) Arnaud, F.; Lignier, V.; Revel, M.; Desmet, M.; Beck, C.; Pourchet, M.; Charlet, F.;
604 Trentesaux, A.; Tribovillard, N. Flood and Earthquake Disturbance of ²¹⁰Pb
605 Geochronology (Lake Anterne, NW Alps). *Terra Nova* **2002**, *14* (4), 225–232.
606 <https://doi.org/10.1046/j.1365-3121.2002.00413.x>.
- 607 (43) Chevallier, M. L.; Della-Negra, O.; Chaussonnerie, S.; Barbance, A.; Muselet, D.; Lagarde,
608 F.; Darii, E.; Ugarte, E.; Lescop, E.; Fonknechten, N.; Weissenbach, J.; Woignier, T.;
609 Gallard, J.-F.; Vuilleumier, S.; Imfeld, G.; Le Paslier, D.; Saaidi, P.-L. Natural Chlordecone
610 Degradation Revealed by Numerous Transformation Products Characterized in Key French
611 West Indies Environmental Compartments. *Environmental Science & Technology* **2019**, *53*
612 (11), 6133–6143. <https://doi.org/10.1021/acs.est.8b06305>.
- 613 (44) Macarie, H.; Novak, I.; Sastre-Conde, I.; Labrousse, Y.; Archelas, A.; Dolfing, J.
614 Theoretical Approach to Chlordecone Biodegradation. In *Crisis management of chronic*
615 *pollution: contaminated soil and human health*; Boca Raton : CRC Press, 2016; pp 191–
616 209.
- 617 (45) Bocquené, G.; Franco, A. Pesticide Contamination of the Coastline of Martinique. *Marine*
618 *Pollution Bulletin* **2005**, *51* (5–7), 612–619.
619 <https://doi.org/10.1016/j.marpolbul.2005.06.026>.
- 620 (46) Bertrand, J. A.; Abarnou, A.; Bodiguel, X.; Guyader, O.; Reynal, L.; Robert, S. Assessment
621 of Chlordecone Content in the Marine Fish Fauna around the French West Indies Related
622 to Fishery Management Concerns. In *Crisis management of chronic pollution:*
623 *contaminated soil and human health*; Boca Raton : CRC Press, 2016; pp 105–117.
- 624 (47) Jones, P. D.; Harpham, C.; Harris, I.; Goodess, C. M.; Burton, A.; Centella-Artola, A.;
625 Taylor, M. A.; Bezanilla-Morlot, A.; Campbell, J. D.; Stephenson, T. S.; Joslyn, O.;
626 Nicholls, K.; Baur, T. Long-Term Trends in Precipitation and Temperature across the
627 Caribbean: PRECIPITATION AND TEMPERATURE TRENDS ACROSS THE
628 CARIBBEAN. *International Journal of Climatology* **2016**, *36* (9), 3314–3333.
629 <https://doi.org/10.1002/joc.4557>.
- 630 (48) Champion, J. Les Possibilités de Mécanisation En Culture Bananière L. *Fruit*. 1970, pp
631 669–683.
- 632 (49) Mickelson, S. K.; Boyd, P.; Baker, J. L.; Ahmed, S. I. Tillage and Herbicide Incorporation
633 Effects on Residue Cover, Runoff, Erosion, and Herbicide Loss. *Soil and Tillage Research*
634 **2001**, *60* (1–2), 55–66. [https://doi.org/10.1016/S0167-1987\(01\)00170-2](https://doi.org/10.1016/S0167-1987(01)00170-2).

- 635 (50) Beckie, H. J. Herbicide-Resistant Weed Management: Focus on Glyphosate. *Pest*
636 *Management Science* **2011**, n/a-n/a. <https://doi.org/10.1002/ps.2195>.
- 637 (51) Henriques, W.; Jeffers, R. D.; Lacher, T. E.; Kendall, R. J. Agrochemical Use on Banana
638 Plantations in Latin America: Perspectives on Ecological Risk. *Environmental Toxicology*
639 *and Chemistry* **1997**, *16* (1), 91–99. <https://doi.org/10.1002/etc.5620160110>.
- 640 (52) Cattan, P.; Bussière, F.; Nouvellon, A. Evidence of Large Rainfall Partitioning Patterns by
641 Banana and Impact on Surface Runoff Generation. *Hydrological Processes* **2007**, *21* (16),
642 2196–2205. <https://doi.org/10.1002/hyp.6588>.
- 643